

## Femtosecond-pulse distortion in quantum wells

Dai-Sik Kim, Jagdeep Shah, D. A. B. Miller, and T. C. Damen  
*AT&T Bell Laboratories, Holmdel, New Jersey 07733*

Wilfred Schäfer

*Hochleistungsrechenzentrum Forschungszentrum, Jülich, W-5170 Jülich, Federal Republic of Germany*

L. Pfeiffer

*AT&T Bell Laboratories, Murray Hill, New Jersey 07974*

(Received 9 September 1993)

We show that a low-intensity femtosecond pulse is severely distorted while propagating through a relatively thin ( $< 7000 \text{ \AA}$ ) GaAs multiple-quantum-well sample and that this pulse distortion depends critically on the dephasing time  $T_2$  and the total thickness  $l$ . An interferometric measurement reveals the existence of well-defined nodes at which the envelope function changes its sign. This pulse distortion significantly affects femtosecond experiments such as pump-probe or four-wave-mixing experiments.

In most studies of semiconductors and their nanostructures using ultrafast spectroscopy, the results are analyzed assuming that the sample is *optically thin*, i.e.,  $\alpha l \ll 1$ , where  $\alpha$  is the absorption coefficient. With this assumption, pulse distortion can be ignored, making theoretical analysis much more manageable. However, the actual samples are very often *optically thick*; for instance, typical GaAs and GaAs multiple-quantum-well (MQW) samples used in transmission experiments are a few thousand  $\text{\AA}$  thick, making  $\alpha l > 1$ . In such optically thick samples, significant pulse distortion is possible, especially when the pulse is shorter than  $T_2$ .<sup>1-4</sup> In GaAs quantum wells, the effects of group-velocity dispersion and hole burning on pulse propagation was studied, but due to the limited time resolution ( $> 9 \text{ ps}$ ) and large inhomogeneous broadening, very little pulse distortion was observed.<sup>5</sup> Interesting results on pulse-breaking effects have been reported for *high-intensity* pulses with long propagation distances.<sup>6,7</sup> With the wide use of femtosecond lasers, the distortion becomes much more important especially around the exciton resonances where the pulse width is smaller than  $T_2$ , and therefore, has to be considered *carefully* in all experiments but in *extremely* thin samples. However, in most transmission experiments, a *time-integrated* signal is measured as a function of the *time delay* between the two pulses. Only recently, the time evolution of four-wave-mixing (FWM) signals has begun to provide considerable new information.<sup>8-13</sup>

In this paper, we demonstrate that a *low-intensity* ultrashort pulse propagating through a typical MQW sample ( $l$  approximately equal to a few thousand  $\text{\AA}$ ) shows *severe* pulse distortions that depend strongly on  $T_2$  (and, therefore, homogeneous linewidth) and laser wavelengths. By comparing different samples, we show that the distortion increases dramatically with  $l$  but decreases with an increase in the inhomogeneous linewidth. Furthermore, using interferometric techniques, we probe the pulse envelope function that shows aperiodic oscillations and well-defined nodes at the exciton resonance. This demon-

strates that the origin of the pulse distortion is reradiation of induced dipoles. The first principle, microscopic, coupled Maxwell-semiconductor Bloch equations (MSBE) calculation shows excellent agreements with the experiments. We also show, by *time resolving* the pump-probe experiments (TR-PP) that the pump-induced change in  $T_2$  is a *primary* factor in the pump-probe experiments, because the pulse distortion is sensitive to  $T_2$ . This gives rise to a net signal which competes with the bleaching. This is in contrast to the predictions of the theory for an infinitely thin sample that there is only broadening of the levels from this effect, so that the structurally integrated total absorption is conserved and the net differential absorption is zero.<sup>14-17</sup>

The experiments were performed on four GaAs MQW samples with their substrates removed. The nominal well width ( $L_z$ ) and periods ( $N$ ) of these samples are 170  $\text{\AA}$ , 10 for sample *A*, 170  $\text{\AA}$ , 15 for sample *B*, 100  $\text{\AA}$ , 65 for sample *C*, and 84  $\text{\AA}$ , 75 for sample *D*. Samples *A* and *B* have small linewidths ( $< 1 \text{ meV}$ ), with FWM decay constant  $\tau_{\text{decay}} = 0.5-0.75 \text{ ps}$  at 10 K so that the homogeneous linewidths is bigger than 0.45 (Ref. 12) ( $T_2 = 2\tau_{\text{decay}}$  for a homogeneously broadened line), whereas samples *C* and *D* are inhomogeneously broadened at low temperatures [linewidth = 3 meV (*C*), 1.8 meV (*D*),  $\tau_{\text{decay}} > 2 \text{ ps}$ ;  $T_2 = 4\tau_{\text{decay}}$ ] and low density. A passively mode-locked, tunable Ti-sapphire laser with 150-fs pulses (10-meV bandwidth) was used to perform transmission and pump-probe experiments at various temperatures, detuning, and photoexcitation densities per layer (between  $3 \times 10^5$  and  $3 \times 10^{10} \text{ cm}^{-2}$ ). Temporal evolution of the transmitted probe beam was obtained using up-conversion techniques.

Figure 1(a) shows the measured temporal evolution of the probe pulse (in the absence of pump) after transmission through samples *A* and *B* at 10 K. The laser is tuned to the heavy-hole exciton resonance. Following the initial peak is a long tail, one to two orders of magnitudes

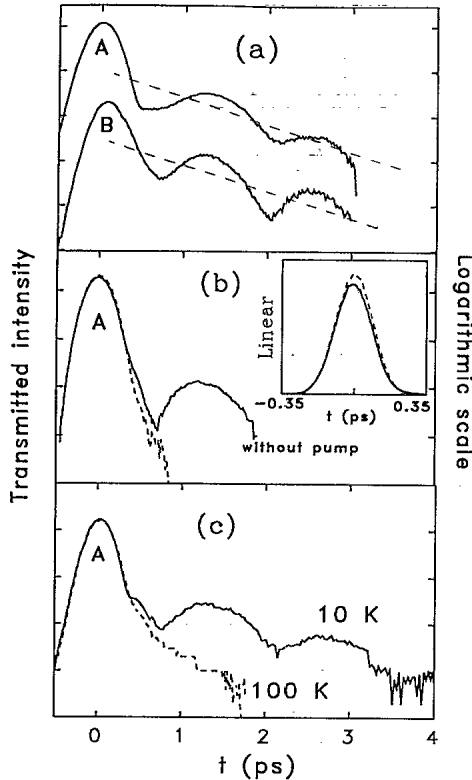


FIG. 1. (a) Transmitted intensity plotted on a logarithmic scale at a low-density limit for sample *A* and *B* and (b) the effect of the pump ( $2 \times 10^{10} \text{ cm}^{-2}$ ) on the shape of the probe for sample *A* at 10 K. (c) The solid curve is taken at 10 K and the dotted curves at 100 K, both without any pump. The laser is centered at heavy-hole exciton resonances.

lower in intensity, that exhibits beats roughly corresponding to the heavy- and light-hole (H-LH) exciton splitting (4 meV). These beats are superimposed on exponential decays (broken lines) whose time constants agree well with  $\tau_{\text{decay}}$  for identical conditions. These tails can be interpreted as the usual free-induction decay (FID).<sup>1,2</sup> As an aside we note that such time-resolved transmission can be measured with good signal-to-noise ratio for excitation densities down to  $\sim 3 \times 10^5 \text{ cm}^{-2}$ , so that  $T_2$  can be determined at densities not accessible with other techniques. Unfortunately, the decay times determined this way reflect the dephasing time directly only for homogeneously broadened samples, unlike the case of resonant Rayleigh scattering where the decay time is independent of the inhomogeneous broadening.<sup>18</sup>

Figure 1(b) shows how the transmitted pulse shape is modified for sample *A* by a pump pulse at  $t = -20$  ps (time delay  $\tau = 20$  ps) producing  $2 \times 10^{10} \text{ cm}^{-2}$ . Figure 1(c) shows the transmitted pulse shape for sample *A* at 10 K (solid curve) and at 100 K (dotted curves), with excitation centered at the heavy-hole exciton at both temperatures. One effect of the pump pulse or a temperature increase is to shorten the tail [Figs. 1(b) and 1(c)]. On the other hand, the linear plot of Fig. 1(b) [inset of Fig. 1(b)] around the peak shows the pump-induced bleaching that is not apparent in the semilogarithmic plot. It is well known<sup>19,20</sup> that an increase of exciton and free-carrier

population, or of temperature, leads to a reduction in the exciton dephasing time  $T_2$ . Since the FID is expected to be shortened by a decrease in  $T_2$ , it is reasonable to conclude that the observed changes in the tail in Figs. 1(b) and 1(c) result from a change in  $T_2$ . This effect, which opposes the bleaching, is relatively small since sample *A* is "thin" with relatively small distortion.

In contrast to samples *A* and *B*, the transmitted pulse shapes in samples *C* and *D* show much more distortion. Figure 2(a) shows the transmitted probe pulse shape (no pump) for samples *C* and *D* at 10 K, with the laser centered on the HH exciton. The transmitted pulse shows distortions that are comparable or even bigger than the initial peak. Also, the oscillations are aperiodic and unrelated to the HH-LH splitting (about 10 meV in these samples). The overall decay rate for samples *C* and *D* is determined by the inhomogeneous exciton linewidth and is faster than the dephasing rate. Sample *D* has significantly more distortions than sample *C*, although  $l$  is slightly smaller than sample *C* because *C* has a larger linewidth and thus more inhomogeneous broadening. This interpretation is supported by our experiments in *n*-doped GaAs quantum wells, where the pulse distortion is minimal because the system is intrinsically inhomogeneously broadened.<sup>11</sup> Here, the polarization decays with a

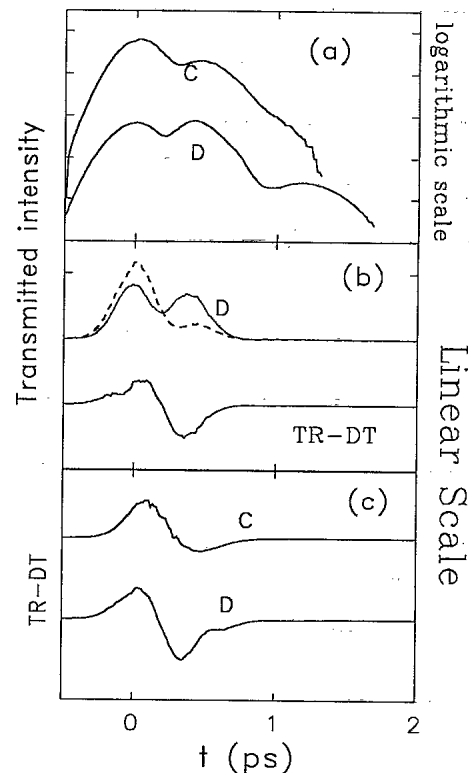


FIG. 2. (a) Semilogarithmic plot of the transmitted intensity of probe at low density ( $2 \times 10^8 \text{ cm}^{-2}$ ) for samples *C* and *D*, without any pump, at 10 K. (b) The solid curve is taken without the pump and the dashed curve represents the pulse shape with the pump on at  $t = -20$  ps, for example *D*. The subtraction of the solid curve from the dashed one is plotted at the bottom, which is the TR-PP. (c) TR-PP for samples *C* and *D* at 10 K and pump intensity of  $2 \times 10^{10} \text{ cm}^{-2}$ .

time constant comparable to the inverse spectral linewidth, which is comparable to the pulse width.

The transmitted pulse shapes for sample *D* at 10 K are shown in Fig. 2(b) without pump (solid curve) and with a pump pulse ( $\tau=20$  ps) producing  $2 \times 10^{10} \text{ cm}^{-2}$ . The effect of the pump pulse is to decrease the secondary emission and increase the main peak, as in sample *A*. However, since the pulse distortions are stronger in sample *D*, so are the changes induced by the pump pulse. The difference in the transmitted intensity with (*T*) and without pump (*T*<sub>0</sub>) for sample *D* [bottom of Fig. 2(b)] shows that the net result of the pump pulse is a *bleaching* (positive *T-T*<sub>0</sub> or TR-PP) followed by induced absorption. Analysis of the curve shows that, for the conditions investigated, there is a 5% net induced absorption, a result that is supported by pump-probe experiments under identical conditions. Figure 2(c) shows TR-PP for samples *C* and *D*, excited at the HH exciton resonance at 10 K, induced by a pump pulse ( $n_s=2 \times 10^{10} \text{ cm}^{-2}$ ,  $\tau=20$  ps). These data show the general trend from primarily a bleaching signal for thin samples (*A* and *B*) to a bleaching followed by induced absorption for thicker samples (*C* and *D*).

We, furthermore, put the sample in one arm of the modified Michelson interferometer so that the interference pattern is obtained between the nondistorted pulse and the pulse that is distorted as a result of passing through the sample [Fig. 3(a)]. The resulting pattern closely resembles the actual envelope function of the distorted pulse. Figure 3(a) shows the interference pattern between the original and the distorted pulses for sample

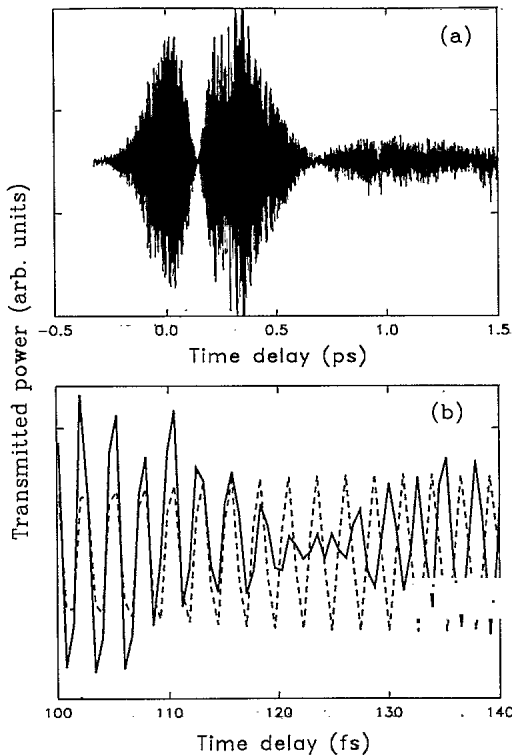


FIG. 3. (a) Interference pattern for resonant (HH) excitation of sample *D* at 10 K. (b) Closer examination of the nodal region. The broken lines are fit to a sinusoidal wave, showing a  $180^\circ$  phase shift at the node.

*D* resonantly excited at the HH resonance at 10 K, with two nodes clearly visible. Closer examination of the first nodal region [Fig. 3(b)] reveals the change of sign (or  $180^\circ$  phase change) at the node where the dotted lines are fitted of the prenodal interference patterns to a sinusoidal wave. The abruptness and unevenness of the sinusoidal fit comes from having only four points per cycle. With the sample removed, and with the appropriate adjustment of the delay, neither the nodes nor the phase shift are present. The phase shift comes from the fact that, at resonance, the polarization is  $90^\circ$  out of phase with the incident radiation, and the reradiation from this induced polarization is another  $90^\circ$  out of phase. A slight detuning of the laser from the resonance shows that, indeed, the rear part of the pulse has the frequency of the exciton resonance, whereas the frequency of the frontal part is determined by the center laser frequency. These results demonstrate unequivocally that the origin of the pulse distortion is the reradiation from the induced polarization.

To understand our results quantitatively, we have performed calculations using microscopic coupled MSBE.<sup>6,21</sup> In this approach, the SBE are solved for the first well with the input pulse as a source, whose solution (the induced polarization) enters the Maxwell equation. The resulting electric field, which is slightly distorted, enters the next well to become the source of the SBE and so on. This way the propagation effect is self-consistently introduced because the electric field is now a combination of the external field and the reradiated field by the induced polarization. Polariton effects, considered earlier for the case of  $\text{Cu}_2\text{O}$ ,<sup>3</sup> are inherent in this approach because of the nature of the coupled equations so that in case of bulk, this method leads to the classical polariton.

Figure 4(a) shows the logarithmic plot of the transmit-

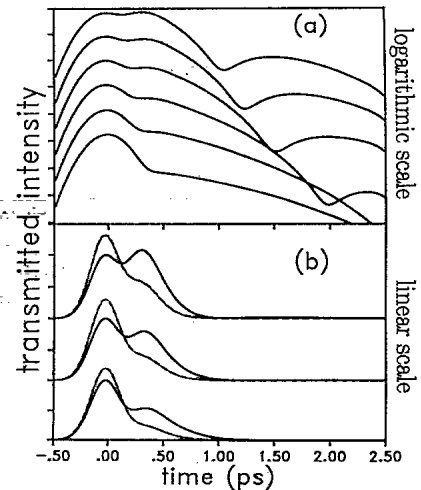


FIG. 4. (a) A logarithmic plot of the theoretical (using MSBE) transmitted intensity of 150-fs pulses resonantly exciting the HH excitons.  $T_2$  and the inhomogeneous broadening are assumed to be 10 ps and 3 meV, respectively. The absorption coefficient is assumed to be  $8 \times 10^4 \text{ cm}^{-1}$  and *l* from top to bottom are 6000, 5000, 4000, 3000, 2000, and 1000 Å, respectively. (b) The effect of reduced  $T_2$  (330 fs) on the pulse shape (broken curves) for  $l=6000$ , 5000, and 4000 Å, along with the linear plots of those assuming  $T_2=10$  ps (solid lines).

ted intensity of 150-fs pulses resonantly exciting the HH resonance.  $T_2$  and the inhomogeneous broadening are assumed to be 10 ps and 3 meV, respectively. The theoretical absorption coefficient is  $8 \times 10^4 \text{ cm}^{-1}$  and  $l$  from top to bottom are 6000, 5000, 4000, 3000, 2000, and 1000 Å, respectively. These curves correctly reproduce the aperiodic oscillations of sample *D*. Figure 4(b) describes the effect of reduced  $T_2$  (330 fs) on the pulse shape (broken curves) for  $l=6000, 5000,$  and  $4000 \text{ Å}$ , which closely resembles the experimental results of Fig. 2(b), including the decrease in the total transmitted power, and thus net induced absorption.

Although we have focused our discussion on the effect of pulse distortion on the pump-probe experiments at HH exciton resonance, it is clear that the distortion can have a significant effect in other femtosecond experiments at different excitation conditions. For instance, the dependences of the pulse distortion and TR-PP results on laser photon energy are in good agreement with our picture and can be compared with the spectrally resolved PP experiments. The time evolution of the FWHM signal in sample *C* (not shown) shows strong oscillations even when only the HH excitons are excited. This would be difficult to explain without knowing that the pulse shape itself is severely distorted. Our results and conclusions point to the need of using coupled MSBE that naturally contains the propagation effect as well as developing a

proper treatment of carrier-density-dependent dephasing as an integral part of SBE. A potentially interesting point is the effect of these distorted pulses on the exciton population. Since the envelope functions of these pulses can have different signs in different regions, emission as well as absorption can occur and the exciton density may have an interesting spatiotemporal dependence.

In conclusion, we have shown that a low-intensity femtosecond laser pulse is severely distorted while propagating through a typical MQW sample, especially in the vicinity of the exciton resonances. This distortion comes from the interference between the laser field and the reradiated field of the induced dipoles. It depends strongly on the dephasing time so that pump-induced change in the dephasing time, an effect heretofore ignored, is a primary factor in pump-probe experiments, and leads to *net induced absorption* for moderately thick quantum wells. Our results show that pulse distortion effects must be considered in the interpretation of pump-probe and other femtosecond experiments. Intensity and energy-dependent dephasing rates should be included in a self-consistent manner in the SBE as well as the pulse distortion for a proper interpretation of ultrafast transient experiments in semiconductors.

We thank J. P. Gordon, E. P. Ippen, W. H. Knox, P. Planken, and P. Y. Yu for helpful discussions.

- <sup>1</sup>H.-J. Hartmann and A. Laubereau, *J. Chem. Phys.* **80**, 4663 (1984).
- <sup>2</sup>A. Laubereau and W. Kaiser, *Rev. Mod. Phys.* **50**, 607 (1978).
- <sup>3</sup>D. Fröhlich, A. Kulik, B. Uebbing, A. Mysyrowica, V. Langer, H. Stolz, and W. von der Osten, *Phys. Rev. Lett.* **67**, 2343 (1991).
- <sup>4</sup>A. Puri and J. L. Birman, *Phys. Rev. A* **27**, 1044 (1983).
- <sup>5</sup>J. Hegarty, *Phys. Rev. B* **25**, 4324 (1982).
- <sup>6</sup>P. A. Harten, A. Knorr, J. P. Sokoloff, F. Brown de Colstoun, S. G. Lee, R. Jin, E. M. Wright, G. Khitrova, H. M. Gibbs, S. W. Koch, and N. Peyghambarian, *Phys. Rev. Lett.* **69**, 852 (1992).
- <sup>7</sup>S. W. Koch, A. Knorr, R. Binder, and M. Lindberg, *Phys. Status Solidi B* **173**, 177 (1992).
- <sup>8</sup>L. Schultheis, M. D. Sturge, and J. Hegarty, *Appl. Phys. Lett.* **47**, 995 (1985).
- <sup>9</sup>M. C. Webb, S. T. Cundiff, and D. G. Steel, *Phys. Rev. Lett.* **66**, 934 (1991).
- <sup>10</sup>G. Noll, U. Siegner, S. Shevel, and E. O. Göbel, *Phys. Rev. Lett.* **64**, 792 (1990).
- <sup>11</sup>D. S. Kim, J. Shah, J. E. Cunningham, T. C. Damen, S. Schmitt-Rin, and W. Schäfer, *Phys. Rev. Lett.* **68**, 2838 (1992).
- <sup>12</sup>D. S. Kim, J. Shah, T. C. Damen, W. Schäfer, F. Jahnke, and S. Schmitt-Rink, *Phys. Rev. Lett.* **69**, 2725 (1992).
- <sup>13</sup>S. Weiss, M.-A. Mycek, J.-Y. Bigot, S. Schmitt-Rink, and D. S. Chemla, *Phys. Rev. Lett.* **69**, 2685 (1992).
- <sup>14</sup>C. H. Brito Cruz, J. P. Gordon, P. C. Becker, R. L. Fork, and C. V. Shank, *IEEE J. Quantum Electron.* **24**, 261 (1988).
- <sup>15</sup>W. H. Knox, in *Hot Carriers in Semiconductors Nanostructures*, edited by J. Shah (Academic, New York, 1992).
- <sup>16</sup>R. Binder, S. W. Koch, M. Lindberg, W. Schäfer, and J. Jahnke, *Phys. Rev. B* **43**, 6520 (1991), and references therein.
- <sup>17</sup>M. Joffre, D. Hulin, A. Migus, and A. Antonetti, C. Benoit à la Guillaume, N. Peyghambarian, M. Lindberg, and S. W. Koch, *Opt. Lett.* **13**, 276 (1988).
- <sup>18</sup>H. Stolz, *Adv. Solid State Phys.* **31**, 219 (1991).
- <sup>19</sup>D. S. Kim, J. Shah, J. E. Cunningham, T. C. Damen, W. Schäfer, M. Hartmann, and S. Schmitt-Rink, *Phys. Rev. Lett.* **68**, 1006 (1992).
- <sup>20</sup>L. Schultheis, J. Kuhl, A. Honold, and C. W. Tu, *Phys. Rev. Lett.* **57**, 1635 (1986).
- <sup>21</sup>W. Schäfer and K. Henneberger, *Phys. Status Solidi B* **159**, 59 (1990).